Mine Water Environ (2009) 28:15–29
DOI 10.1007/s10230-008-0059-z

TECHNICAL ARTICLE

Physico-chemical gradients and meromictic stratification in Cueva de la Mora and other acidic pit lakes of the Iberian Pyrite Belt

Javier Sánchez España · Enrique López Pamo · Marta Diez · Esther Santofimia

Received: 24 September 2008 / Accepted: 12 December 2008 / Published online: 8 January 2009
© Springer-Verlag 2009

Abstract A marked vertical trend of increasing temperature and dissolved metal concentrations is observed in the monimolimnia of some meromictic pit lakes of the Iberian Pyrite Belt (IPB) in SW Spain. Temperature differences between the chemocline and the pit lake bottom can be as high as 15°C (e.g. Herrerías), and the respective concentration of some metals (e.g. Fe) and metalloids (e.g. As) can increase by several orders of magnitude (e.g. Cueva de la Mora). The redox conditions also change drastically from the upper and oxygenated mixolimnion (strongly oxidizing) to the lower and anoxic monimolimnion (moderately reducing). Processes such as the inflow of metal–sulphate laden ground water from flooded shafts and galleries, and other factors such as the pit geometry or the relative depth of the lakes, must be considered to account for the observed stratification pattern. The vertical profiles of physico-chemical parameters and water chemistry obtained in Cueva de la Mora and other meromictic pit lakes of the IPB are also compatible with a reactive bottom in which several geochemical and microbial reactions (including reductive dissolution of Fe^{3+} minerals, bacterial reduction of Fe^{3+} and SO_4^{2-} in pore waters within the sediments, and decomposition of organic matter) could be taking place.

Keywords Acid mine drainage · Double-diffusive convection · Geochemistry · Meromixis · Pit lake · Spain

J. S. España (✉) · E. L. Pamo · M. Diez · E. Santofimia
Instituto Geológico y Minero de España (IGME), Alenza, 1, 28003 Madrid, Spain
e-mail: j.sanchez@igme.es

Introduction

A long history of mining in the Iberian Pyrite Belt (IPB) massive sulphide district (in SW Spain) has left an inheritance of abandoned mines (mainly in the province of Huelva) and a large number of waste piles, tailings impoundments, and flooded pits. This represents one of the world's largest accumulations of mine wastes and acid mine drainage (AMD; Sánchez-España et al. 2005a). The mineralogical and textural characteristics of the IPB ores (with a dominantly pyritic, fine-grained and highly reactive mineralization and a lack of carbonates; Sáez et al. 1999; Sánchez-España 2000; Tornos 2006) has favoured the oxidation and dissolution of pyrite and the subsequent formation of AMD (Sánchez-España et al. 2005a). These mine waters have caused severe pollution of acidity and dissolved metals (Fe, Al, Mn, Cu, Zn, Cd, Pb), As, and SO_4 to the Odiel and Tinto river systems (Braungardt et al. 2003; Olías et al. 2004; Sánchez-España et al. 2005a, 2006a; Van Geen et al. 1991). This acidity and metal pollution has caused the loss of most forms of aquatic life, and only acidophilic microorganisms (both eukaryotic and prokaryotic) inhabit these extreme environments (e.g. Aguilera et al. 2006; González-Toril et al. 2003; López-Archilla and Amils 1999; López-Archilla et al. 2001; Rowe et al. 2007).

Most of the mine pits developed in the IPB during the twentieth century were abandoned in the 1980s and 1990s. These mine voids were progressively flooded by the entrance of direct rainfall, runoff, ground water and mine drainage from nearby galleries and waste piles. At present, more than 20 pit lakes with highly acidic water containing high metal and sulphate concentrations exist in the provinces of Huelva and Sevilla (Sánchez-España et al. 2008a). Combined, these pit lakes contain around 25 × 10^6 m^3 of

AMD. Some pits (e.g. Corta Atalaya) are still in a flooding phase; therefore, the total volume of AMD will increase in the future.

In general, the pit lakes of the IPB are very diverse in size, depth, age, and water composition, but share a common geological framework. The great majority of the pit lakes are meromictic and show a permanent stratification with a chemocline separating an upper, oxygenated and lower-density mixolimnion from a lower, anoxic and higher-density monimolimnion, which is perennially isolated from the rest of the water column. The mixolimnion can be very thin (as in Confesionarios or N^{a}S^{a} del Carmen, where it is only 2–3 m deep), or may show chemical and physical gradients over a depth range on the order of tens of meters (e.g. 30 m in San Telmo or 10 m in Cueva de la Mora). As regards to the monimolimnia, recent research (Sánchez-España et al. 2007a, 2008a, b) has revealed the existence of two distinct stratification patterns. Type I lakes, represented by San Telmo or N^{a}S^{a} del Carmen, have a chemically uniform monimolimnion with no vertical gradients. In contrast, the monimolimnia of Type II lakes, exemplified by Cueva de la Mora, Herrerías or Filón Centro (Tharsis), shows marked vertical changes in physico-chemical parameters, with decreasing redox potential, and increasing temperature, pH and dissolved solids content with depth.

Recent morphometric observations based on airborne photography and depth profiles (IGME 2008; Sánchez-España et al. 2008a) suggest that the different types of hydrochemical stratification in the IPB pit lakes could be related to geometric factors, such as the pit geometry and relative depth (here, the relative depth was defined as $z_r = \frac{50 z_m \sqrt{\pi}}{\sqrt{A0}}$, where z_m = maximum depth and A_0 is the lake surface area; Wetzel 2001). A summary of the available morphometric data for selected pit lakes of the IPB is provided in Table 1. Type I lakes usually show an oval surface area [with a (major axis)/(minor axis) ratio ≈ 1.2–1.4] and very high relative depths (ranging from 25 to 45%). On the other hand, Type II lakes usually show a more elongated, ellipsoidal surface area [(major axis)/(minor axis) up to 3.0] and similarly high relative depths (in the range of 18–50%), although there are also exceptions to this general rule. There are no significant differences between both types of lakes as regards to their volumes or ages (Table 1).

In a previous paper (Sánchez-España et al. 2007a), a hydrogeochemical and microbiological description of a Type I pit lake was presented for the San Telmo mine site. The present paper is the first report of the main physico-chemical characteristics observed in the monimolimnia of the Type II pit lakes, mainly through observations from Cueva de la Mora and other meromictic pit lakes of the IPB such as Herrerías, Filón Centro (Tharsis), and Confesionarios (Fig. 1). The information provided in this paper includes recent limnological and hydrogeochemical data

Table 1 Summary of morphometric data for selected pit lakes of the Iberian Pyrite Belt (modified from Sánchez-España et al. 2008 and IGME 2008)

Pit lake	Age (years)	Max ∅ (m)	Min ∅ (m)	(Max ∅/ Min ∅)	Area (hm^2)	Max depth (m)	Rel depth (%)	Volume (hm^3)	Stratification type
Corta Atalaya	4	300	150	2.00	4.70	70	28.61	1.4	Meromictic ?
Filón Sur (Tharsis)	?	65	50	1.30	0.20	5	9.91	0.01	Meromictic ?
Filón Centro (Tharsis)	40	430	140	3.07	3.80	40	18.18	0.6	Meromictic (type II)
Confesionarios	120	200	160	1.25	2.48	80	45.02	1.0	Meromictic (type I)
Ntra. Sra. del Carmen	?	110	80	1.38	0.70	32	33.90	0.1	Meromictic (type I)
Peña del Hierro	42	200	120	1.67	1.87	>50	–	–	Meromictic
La Zarza-E	12	220	100	2.20	0.70	>40	–	–	Meromictic ?
La Zarza-W	12	240	100	2.40	0.77	>40	–	–	Meromictic ?
Cueva de la Mora	>60	300	90	3.33	1.78	40	26.57	0.3	Meromictic (type II)
Herrerías I (Guadiana)	42	110	90	1.22	0.81	50	49.23	0.2	Meromictic (type II)
San Telmo	16	510	380	1.34	14.36	107	25.02	7.0	Meromictic (type I)
Concepción	>30	280	60	4.67	1.20	15	12.14	0.4	Meromictic ?
Angostura	>70	110	90	1.22	0.84	>40	–	–	Meromictic ?
Tinto and Santa Rosa	77	160	80	2.00	1.11	23	19.35	0.1	Meromictic (type II)
Aznalcóllar	13	850	400	2.13	28.40	38	6.32	6.0	Holomictic
Herrerías II (Santa Barbara)	42	230	90	2.56	1.42	15	11.16	0.10	Holomictic
Los Frailes	7	460	280	1.64	13.30	105	25.52	6.30	Holomictic

Morphometric data: maximum diameter (max ∅), minimum diameter (min ∅), [max ∅/min ∅] ratio, area, maximum depth (max depth), relative depth (rel depth), volume. The age of the pit lake (considering the beginning of the flooding phase) and the stratification type is also provided

Fig. 1 Photographs of the acidic mine pit lakes discussed in the present paper: **a** Cueva de la Mora, **b** Guadiana (Herrerías), **c** Filón Centro (Tharsis), **d** Confesionarios

that were used to compare the water chemistry and the stratification patterns among different pit lakes with distinct size, age, geometry, and depth. Based on the field data, preliminary ideas are presented about the possible physical, geochemical, and microbial controls on the pit lake water compositions and their temporal evolution. The results of these investigations could serve in the future to aid mining companies or regulatory agencies in the design of remediation/restoration alternatives.

Methods

Field measurements and sampling

The field and analytical data correspond to several sampling periods conducted between 2006 and 2008. Depth measurements and vertical profiles of pH, Eh, temperature (*T*), dissolved O_2 (DO), specific conductivity (SC), and chlorophyll-a concentration were collected with a Hydrolab® Datasonde S5 probe from the Hach Company. The concentration of Fe(II) was measured by reflectance photometry with a Merck RQflex10 reflectometer and Reflectoquant® analytical strips. Two different reagents were used depending on the Fe(II) concentration: (1) Ferrospectral® for $0.5 \text{ mg/L} < \text{Fe(II)} < 20 \text{ mg/L}$, and (2) 2,2′-bipiridine for $20 \text{ mg/L} < \text{Fe(II)} < 200 \text{ mg/L}$. Some samples had to be previously diluted with acidified distilled water. Acidity titrations were also performed on site in two samples of the Cueva de la Mora pit lake (corresponding to waters from the surface and the deepest part of the lake). These titrations were carried out with a Hanna portable pH meter using an HI 9025 electrode properly calibrated against supplied standards (Hanna standard solutions HI 7004 for pH 4.01, and HI 7007 for pH 7.01). To ensure total oxidation of the ferrous iron present in the samples, a few drops of H_2O_2 were previously added to the samples. After agitation for 5 min at 30°C, 1.6 N NaOH was progressively added to the samples and both the pH and the mass of added solution were continuously measured to a pH endpoint of 8.3.

Lake water samples were collected with either 60 mL-syringes from the water surface or with an opaque, 2.2 L-capacity, BetaPlus® PVC bottle from Wildlife Supply Company to obtain water samples at different depths. All samples were filtered on site with 0.45 μm membrane filters from Millipore, stored in 125 mL polyethylene bottles, acidified with HNO_3, and refrigerated at 4°C during transport.

Laboratory analyses

Water samples were analyzed by atomic absorption spectrometry (AAS) for Na, K, Mg, Ca, Fe, Cu, Mn, Zn and Al, by inductively coupled plasma-atomic emission spectrometry

(ICP-AES) for Ni, and by inductively coupled plasma-mass spectrometry (ICP-MS) for As, Cd, Co, Cr and Pb. Sulphate was gravimetrically measured as $BaSO_4$. The accuracy of the analytical methods was verified against certified reference waters and close agreement with certified values was achieved for all metals. ^{115}In was used as internal standard for calibration of the ICP-MS analyses. The detection limits for trace elements were 10 μg/L for Zn, 2 μg/L for Ni, Co, Cr and Pb, 0.4 μg/L for As, Cd and Cu. The detection limits for the major cations Na, K, Ca, Mg, Mn, Fe and Al were <1 mg/L in all cases.

Solid samples were analyzed by X-ray fluorescence (XRF) spectrometry (PHILIPS 1404) for the elements Si, Al, Fe, Ca, Mn, and Mg, by an elemental analyzer (Eltra CS-200) for total S, by ICP-MS (after digestion with HNO_3 and H_2O_2) for Cd, Co, Th, U, V, and Zn, and by AAS for Na, Cu, As, and Pb. Certified international reference materials (BCS 175/2, BCS 378, FER-1, FER-2) were used to check the accuracy of the analytical data. The detection limits for trace elements were 10 μg/g for Ni, 2 μg/g for Co, Cu, Th, V, and Zn, and 0.2 μg/g for Cd and U.

The solid samples were washed with pure distilled water to avoid the formation of sulphate salts by evaporation of the interstitial waters during drying. The samples were characterized by X-ray diffraction (XRD) (PHILIPS PW 1710 with CuK_α radiation, 40 kV, 40 mA), scanning electron microscopy (SEM) (PHILIPS XL-30) and energy dispersion spectrometry (EDS) (PV-9900; UAM).

Geochemical modeling

The PHREEQC code (version 2.15; Parkhurst and Appelo 1999) was used for calculation of the saturation index (SI) of the pit lake waters with respect to selected iron and aluminium minerals. Among the databases provided with the PHREEQC software, the file Minteq.v4.dat was selected. This database was enlarged with thermodynamic data (solubility products and enthalpies of formation) for schwertmannite and ferrihydrite given in Bigham et al. (1996).

Results

Cueva de la Mora pit lake

Physico-chemical stratification

The Cueva de la Mora pit lake has a surface area of 17,800 m^2 and a maximum depth of 40 m. This mine was abandoned in the 1940's, and so it represents a mature stage of pit lake development with more than 60 years of hydrogeochemical evolution. At present, the pit lake shows an upper mixolimnion of around 10 m depth, and a lower, 30 m deep monimolimnion, which is sharply stratified and shows several sub-layers of increasing temperature, density, and metal–sulphate concentration towards the lake bottom (Figs. 2, 3). The lake bottom is considerably warmer than the upper monimolimnion (18 and 12–14°C, respectively), and shows significantly higher pH (pH 4.1–4.7 versus 2.7–3.1, respectively). Despite the increase in pH, total acidity increases considerably with depth (e.g. 1,150 mg/L $CaCO_3$ eq. at the surface and 8,400 mg/L $CaCO_3$ eq. at 36 m depth). The bottom waters show a much lower redox potential than the shallow water (200–300 versus 500–700 mV, respectively) and much higher concentrations of dissolved solids, as indicated by the SC (11–12 versus 2–4 mS/cm, respectively). Although the vertical trends of these parameters show slight seasonal variations, the general features remain relatively constant throughout the year.

The vertical distribution of redox potential (Eh) parallels trends in DO and iron speciation (Fig. 3). The redox conditions of the mixolimnion correspond to oxygen-saturated conditions where Fe is predominantly in its oxidized form [$Fe(III) \approx 100\% \ Fe_{total}$], whereas the strongly reducing environment of the monimolimnion is characterized by anoxia and a very high Fe concentration, which is essentially all ferrous iron [$Fe(II) \approx 100\% \ Fe_{total}$]. Interestingly, marked metalimnic peaks of oxygen concentration (with values approaching 12.2 mg/L O_2 and 140% O_2 saturation) were observed in the summer months (e.g. June 2006, July 2007; Fig. 4). These O_2 concentration maxima occur near the thermocline and approach the location of the chlorophyll *a* concentration peaks measured during the same seasons (Fig. 4). This suggests a fundamental microbial control on the mixolimnetic O_2 concentration profile, probably as a result of enhanced photosynthetic activity during this period. Spring is characterized by algal blooms in many natural lakes, where algae are usually accumulated in the metalimnion (Wetzel 2001). This phenomenon was observed in Cueva de la Mora during a study conducted in July 2007. This study revealed a significant number of photosynthetic microorganisms such as green algae and diatoms (Fig. 5). The vertical and seasonal evolution of the algal biomass illustrated in Fig. 4 (as deduced from the chlorophyll-a concentration) may have profound implications for the biogeochemistry of the pit lake. Primary production taking place in the upper lake waters provides a continuous source of organic substances (dissolved organic acids, dead algal and bacterial biomass) for the secondary decomposers (e.g. Fe and S-reducing bacteria), which commonly inhabit the anoxic and reducing lake bottoms (Ehrlich 2002).

The concentration of iron and other elements such as sulphate and arsenic in the pit lake bottom are high in

Fig. 2 Seasonal depth profiles of T, pH, specific conductivity (SC) and Eh in the Cueva de la Mora pit lake obtained in 2006 and 2007

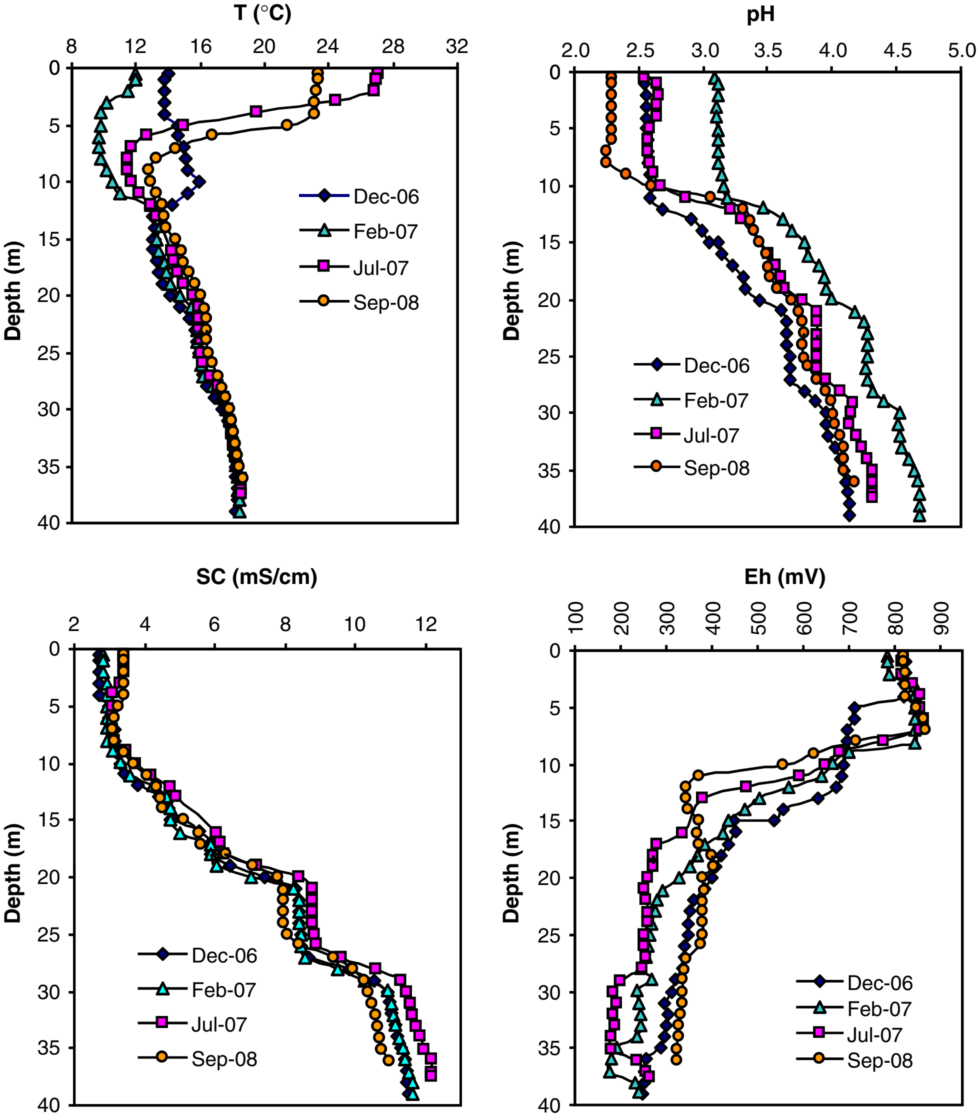

comparison to the mixolimnion (Figs. 6, 7). The most striking examples include Fe (110–130 mg/L in the epilimnion, and approaching 6,000 mg/L in the deepest part of the monimolimnion), SO_4^{2-} (2 g/L in the epilimnion and 13 g/L in the bottom layer), and As (70–120 µg/L in the uppermost layer and 15,000–17,500 µg/L in the bottom layer). Mn and Zn also increase sharply with depth (from 10 to 20 mg/L in the surface to 110–120 mg/L in the lower layer in both cases), and only Al and Cu show a reverse trend, which appears to be related to the precipitation of Al oxyhydroxysulphates (such as alunite and/or basaluminite) at pH 4.0–4.5 along with the subsequent adsorption/coprecipitation of copper. Among the trace metals, Co and Ni also display a vertical trend of increasing concentration with marked differences between the surface and the deepest part of the lake (e.g. from 1,700 to 13,200 µg/L for Co, and from 440 to 850 µg/L for Ni in July 2007; data not shown). On the other hand, other metals like Cd, Cr, and Pb do not show such trends, and the concentrations measured at the surface (e.g. 10–15 µg/L Cd, 20–30 µg/L Cr, 125–150 µg/L Pb) are similar to or slightly higher than those in the deepest layer (e.g. <5 µg/L Cd, <20 µg/L Cr, 10–30 µg/L Pb; data not shown).

Precipitate mineralogy

Sediments taken from the lake shore and floating biofilms sampled from the surface layer were analyzed in July 2007. The chemical and XRD analyses of these ochreous precipitates revealed a predominance of ferric compounds such as jarosite, schwertmannite, and goethite, with lesser amounts of detrital minerals such as quartz, chlorite, muscovite, or feldspar. The occurrence of the three Fe(III) minerals has been widely documented in AMD systems of the IPB (Sánchez-España et al. 2005a, b, 2006a, b) and elsewhere in AMD-affected basins (e.g. Bigham et al.

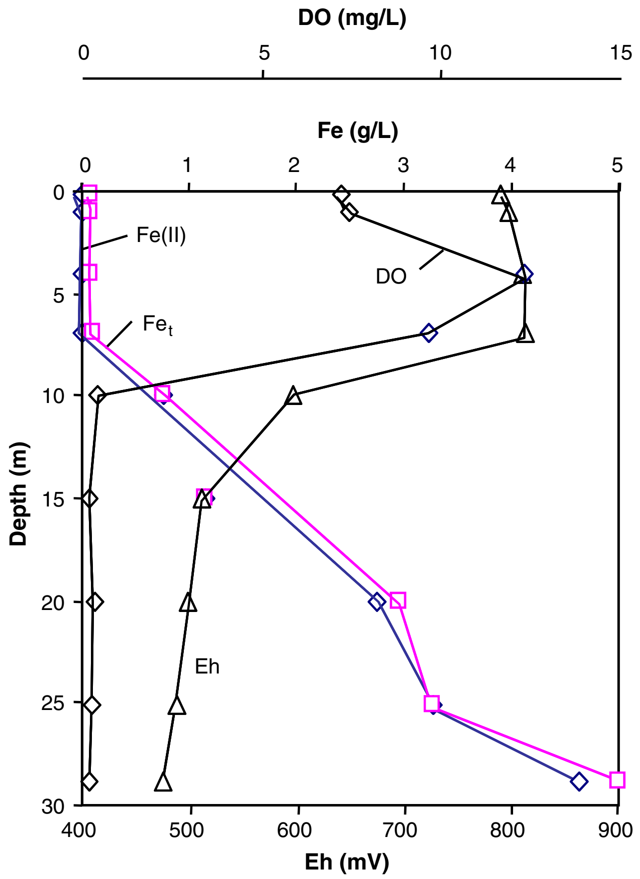

Fig. 3 Depth profiles of dissolved ferrous [Fe(II)] and total (Fe$_t$) iron, dissolved O_2 and Eh in the Cueva de la Mora pit lake. Data from June 2006

1996; Bigham and Nordstrom 2000). Jarosite is commonly favoured at very low pH (of around 2.2 or less), whereas schwertmannite commonly forms in the pH range of 2.5–3.5. Slight changes in the pH of the lake water could have thus caused the formation of these different minerals (the observed pH range in the epilimnion is 2.2–3.1; Fig. 2). Goethite is commonly considered as a product of slow transformation of jarosite and schwertmannite, which are both metastable phases with respect to goethite (Bigham et al. 1996; Bigham and Nordstrom 2000). Therefore, the presence of this mineral could be indicative of the degree of aging or mineralogical maturation of the ochreous precipitates (Sánchez-España et al. 2005a, 2007b).

Geochemical modelling carried out with PHREEQC (Parkhurst and Appelo 1999) confirms the above described mineralogical findings. These calculations indicate oversaturation of the mixolimnion of Cueva de la Mora pit lake with respect to a number of Fe(III)-containing minerals, including schwertmannite, K-, Na-, and H-jarosite, and goethite (Fig. 8a). The high organic content of these solids (up to 1.4 wt% C_{org}) suggests the presence of abundant biomass (algal and/or bacterial cells) and/or adsorbed organic substances on the ferric mineral particles. Allochthonous detritus and organic substances, such as humic acids, resulting from surface runoff, could also be a source of some of this organic carbon.

Schwertmannite is a widespread oxyhydroxysulphate mineral that controls the aqueous concentration of Fe(III) in the acidic mine waters and pit lakes of the IPB in the pH range of 2.5–3.5 (Sánchez-España et al. 2005a, b, 2006a, b, 2008a). The precipitation of this mineral through reaction (1) (Bigham et al. 1996; Bigham and Nordstrom 2000) has been observed to constitute the principal Fe-buffering mechanism in other pit lake regions, such as those of Lusatia, Germany (Regenspurg et al. 2004, Totsche et al. 2003), or Butte, Montana, USA (Gammons and Duaime 2006; Pellicori et al. 2005):

$$8Fe^{3+} + SO_4^{2-} + 14H_2O \Leftrightarrow Fe_8O_8(SO_4)(OH)_6 + 22H^+ \quad (\log K = 18;\ \text{Bigham et al. 1996}) \tag{1}$$

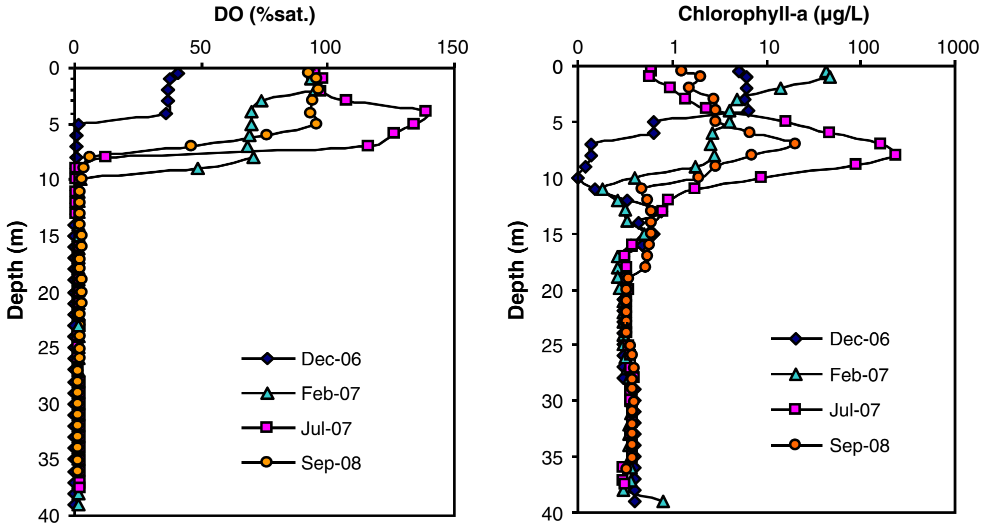

Fig. 4 Seasonal depth profiles of dissolved oxygen (*DO*) and chlorophyll *a* concentration in Cueva de la Mora pit lake obtained in 2006 and 2007

Fig. 5 Photomicrographs of photosynthetic green algae, diatoms and other microorganisms living in the surface waters of the Cueva de la Mora pit lake (water samples taken in July 2007): **a** filamentous green algae of the genus *Zignema* (*Zig*); **b** unicellular and flagellated green algae of the *Chlamydomonas* genus (*Chm*), along with diatoms (long cells; *Dia*) and bacteria (scattered thin bacillus-type cells; *Bac*); **c** diatoms, *Chlamydomonas*, unicellular flagellated cells of *Ochromonas* (*Och*) and bacteria; **d** *Chlamydomonas*. Images taken by confocal microscopy (courtesy de M.A. Aguilera, Centro de Astrobiología, CSIC-INTA)

However, in the anoxic and reducing environment of the monimolimnion, the water becomes undersaturated with respect to all Fe(III) minerals (Fig. 8a). Thus, the saturation index results are compatible with a vertical cycling model for iron, with precipitation in the upper mixolimnion and re-dissolution in the monimolimnion.

In contrast to Fe, PHREEQC computations predict undersaturation of Al-minerals in the mixolimnion and oversaturation in the monimolimnion, which basically results from the pH gradient (pH 2.3–3.1 in the surface and pH 4.1–4.7 near the bottom). In this case, the aluminium solids that appear to be closest to equilibrium saturation are alunite and basaluminite (Fig. 8b). The formation of these two minerals can be described by the following reactions (Bigham and Nordstrom 2000; Nordstrom 1982):

$$3Al^{3+} + K^{+} + 2SO_4{}^{2-} + 6H_2O \leftrightarrow KAl_3(SO_4)_2(OH)_{6(s)} + 6H^{+} \qquad (2)$$

$$4Al^{3+} + SO_4{}^{2-} + 14H_2O \leftrightarrow Al_4(SO_4)(OH)_{10}\cdot 4H_2O_{(s)} + 10H^{+} \qquad (3)$$

Between these two minerals, the SI trends for alunite more closely mimic the vertical trends in Al concentration in solution. Alunite is predicted to begin precipitating (reaction 2) at an approximate depth of around 12 m. This depth is slightly above the level at which the Al concentration begins to decrease (Fig. 6). Basaluminite is not predicted to precipitate (reaction 3) until depths near the lake bottom, where the pH approaches 4.5 (Fig. 8b). Other Al phases, such as gibbsite or amorphous $Al(OH)_3$ (s), are undersaturated at all depths and do not seem to play a significant role in the Al geochemistry of Cueva de la Mora pit lake (Fig. 8b). Jurbanite is apparently near equilibrium in the mixolimnion and saturated in the monimolimnion, although this mineral has not been found as mine drainage precipitate in the IPB province, nor in other AMD systems (Bigham and Nordstrom 2000).

Some secondary sulphate salts like gypsum, pickeringite, and hexahydrite, which are frequently observed as efflorescent minerals on the pit lake shore, have also been sampled and chemically analyzed. The analytical results usually reveal very high contents of trace metals, like Cu (1,200 ppm) and Zn (3,900 ppm), so that the dissolution of these salts during storm events may also affect the trace metal chemistry in the mixolimnion, especially if they occur during mixolimnetic overturn. Adsorption of trace metals onto freshly formed iron minerals, which then

Fig. 6 Seasonal depth-concentration profiles for Fe, SO_4^{2-}, Al, Cu and Zn in the Cueva de la Mora pit lake obtained in 2006 and 2007

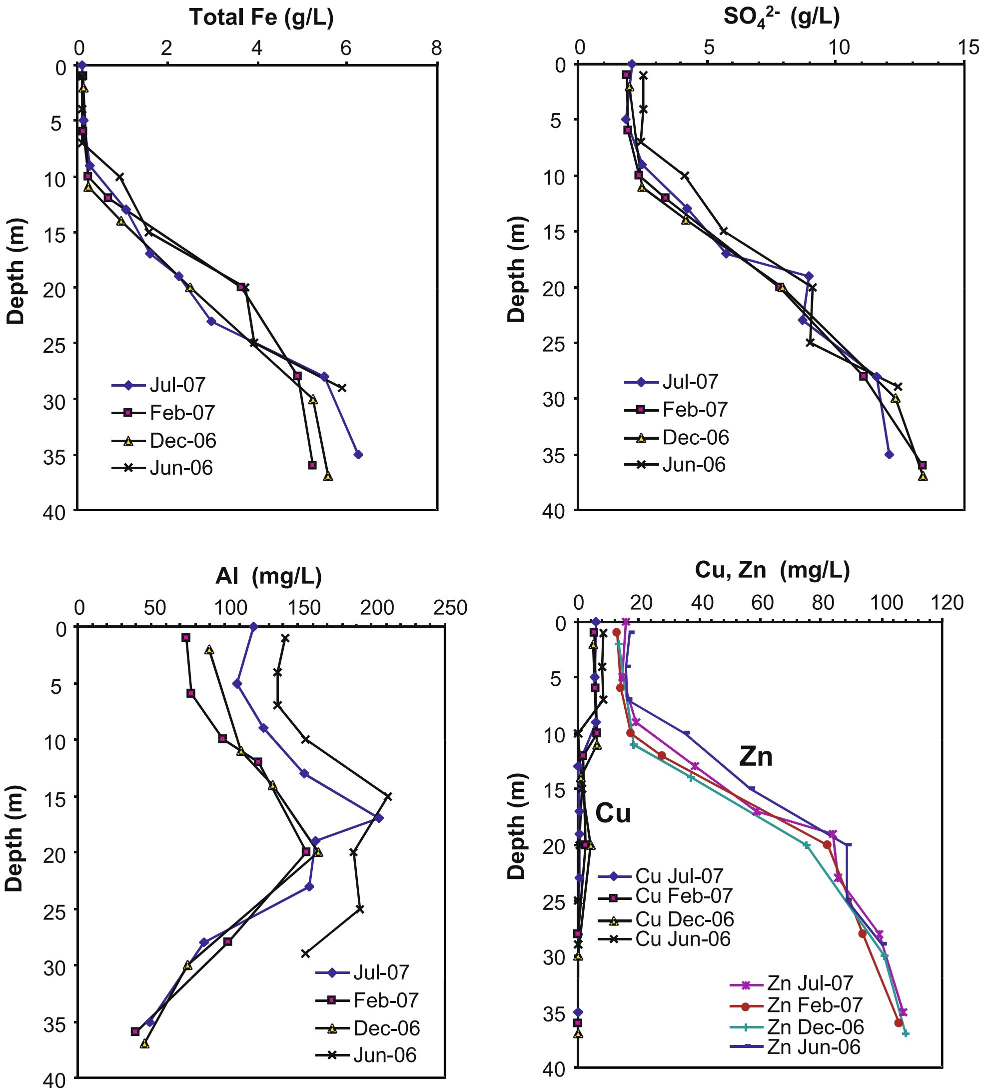

descend by gravity, could result in downwards transport of metals into the monimolimnion and benthic sediment.

Other examples of pit lakes in the Iberian Pyrite Belt

Filón Centro (Tharsis) and Herrerías pit lakes

Morphometric data for the Filón Centro and Herrerías pit lakes are provided in Table 1. Both lakes have a small volume (0.6 and 0.2 hm^2, respectively), moderate surface area (3.8×10^6 and 0.8×10^6 m^2, respectively) and very high relative depth (40 and 50%, respectively). Depth profiles for Filón Centro (Fig. 9) and Herrerías (Fig. 10) show Type II pit lake stratification similar to Cueva de la Mora, with an oxygenated mixolimnion and an anoxic monimolimnion, the latter characterized by an increase in temperature, pH, and total dissolved solids with depth. Indeed, this stratification type seems to be the most abundant type observed to date in the pit lakes of the IPB.

Confesionarios pit lake

The Confesionarios pit lake has a surface area of 24,800 m^2 and a maximum depth of 80 m (Table 1). This lake contains around 1×10^6 m^3 of acidic water with a pH of 2.5–3.5 and high metal and sulphate concentrations (Sánchez-España et al. 2008b). With an estimated age of around 120 years, it is considered the oldest pit lake in the IPB and therefore represents a matured stage within the IPB spectrum. This pit lake shows a thin mixolimnion around 4–5 m deep, and a monimolimnion, which is 75 m deep. The monimolimnion has two different layers: (1) an upper, chemically homogenous layer from 5 m to around 53 m in depth; (2) a lower layer from 53 m to around 80 m depth that shows a steepening gradient of temperature, Eh, and pH towards the bottom (Fig. 11). Although the temperature of the upper monimolimnion is similar to that of the mixolimnion during the winter months (Fig. 11), salinity differences preclude a winter turnover and ensure a

Fig. 7 Seasonal depth-concentration profiles for Mn, Ca, Mg, K, Na, and As in the Cueva de la Mora pit lake obtained in 2006 and 2007

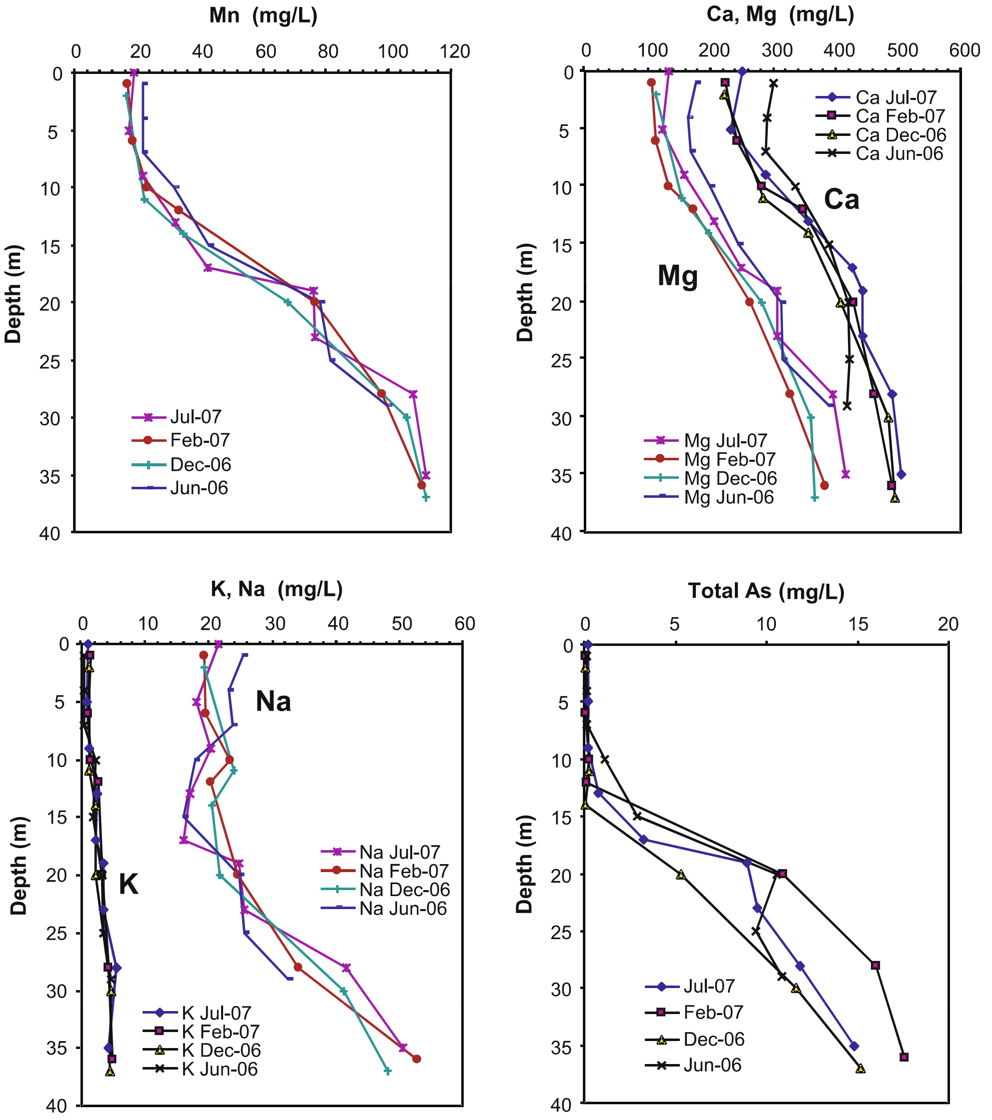

perennial chemical stratification. Both monimolimnetic layers show differences in pH (2.5 in the upper monimolimnion and 2.7–3.4 in the lower monimolimnion), iron speciation, and redox conditions (dissolved iron is predominantly ferric in the upper monimolimnion and chiefly ferrous in the lower monimolimnion; Fig. 11). Such chemical gradients towards the pit lake bottom could be due to upwards diffusion of dissolved constituents from a reactive sediment cover, although this still needs to be checked.

XRD examination of sediments collected from the lake bottom indicates a large quantity of jarosite and goethite, together with abundant detrital minerals like quartz, chlorite, muscovite, kaolinite, and feldspar. The chemical profile obtained for a 25 cm long sediment core taken from the pit lake bottom revealed a clear enrichment in organic carbon at the surface of the sediment cover (up to 1.3% wt. C_{org} in the upper 3 cm of the sediment column). This profile also indicated local sulphur enrichment (6–19 wt% S) between 15 and 20 cm depth, where both pyrite and native sulphur have been detected by XRD. However, further work is needed to determine the origin of these minerals (e.g. detrital or authigenic). The trace metal content of these sediments is generally low (e.g. 50–170 ppm Zn, 45–300 ppm Cu, and <120 ppm Mn), although arsenic is notably enriched (150–1,200 ppm As).

Discussion

The strong redox gradient observed in the studied pit lakes, with low Eh values (100–200 mV) near the pit lake bottom, suggest that some anaerobic reducing reactions could be taking place. These reactions are commonly catalyzed by colonies of anaerobic bacteria that inhabit the water/sediment interface and couple the anaerobic oxidation of

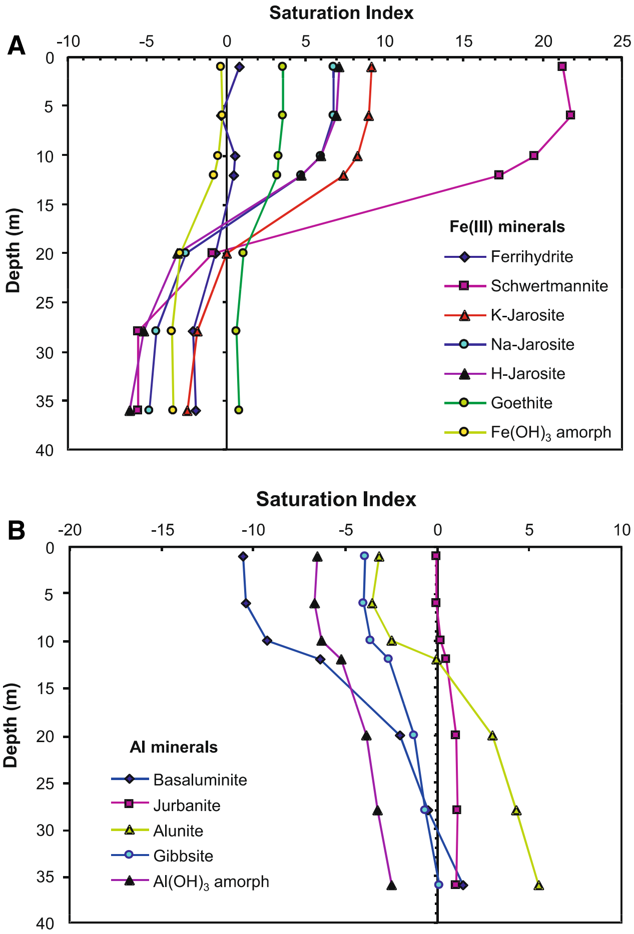

Fig. 8 Vertical trends in the saturation index (SI) of selected Fe(III) minerals (**a**) and Al minerals (**b**) in the pit lake of Cueva de la Mora. Calculations based on water samples collected in July 2007

organic compounds (e.g. decomposing biomass settled from the mixolimnion) with the reduction of oxidized substances, such as Fe^{3+}-containing sediments, Mn^{4+} oxides or dissolved sulphate (Boehrer and Schultze 2008; Schlesinger 2005; Wetzel 2001; reactions 4–6):

$$CH_2O + 2MnO_2 + 4H^+ \rightarrow CO_2 + 2Mn^{2+} + 3H_2O \qquad (4)$$

$$CH_2O + 4Fe(OH)_3 + 8H^+ \rightarrow CO_2 + 4Fe^{2+} + 11H_2O \qquad (5)$$

$$2CH_2O + SO_4^{2-} + 2H^+ \rightarrow 2CO_2 + H_2S + 2H_2O \qquad (6)$$

A common feature of reactions 4 to 6 is that all of them consume protons (thus causing pH to increase if no buffering mechanism, such as reaction 1, exists), and generate CO_2. Given the high hydrostatic pressure prevailing in the deepest layers (up to 4–8 bars, depending on the pit lake depth), the CO_2 remains dissolved and accumulates in the monimolimnion during years or decades. Concentrations of dissolved CO_2 exceeding 0.01 M have been recently confirmed in the monimolimnion of Cueva de la Mora (research in progress), and elevated CO_2 also exists in other pit lakes like Herrerías, Tinto-Santa Rosa, and Filón Centro (Tharsis). In these lakes, the water samples taken from the deepest zones usually show an elevated gas pressure and high density of gas bubbles. The detection of high concentrations of total organic carbon and other biogenic products such as ammonium in the monimolimnion of Cueva de la Mora (e.g. >3 mM TOC and >0.03 mM NH_4^+; research in progress) are also compelling evidence of microbial activity in the anoxic bottom waters of these pit lakes. Although a typical "rotten-egg" smell has been noticed in some water samples taken in Cueva de la Mora, the presence of H_2S has not been demonstrated yet, and therefore, no evidence of sulphate-reducing activity (reaction 6) exists in this lake. Because reactions 4–6 are also slightly exothermic, they could explain, at least in part, some of the temperature increases observed in the deep waters of the pit lakes (see Figs. 2, 9, 10). The reductive dissolution of ferric precipitates such as schwertmannite, jarosite, or goethite (represented by the simplified reaction 5), could also account for some of the observed increases in trace elements such as arsenic, which is

Fig. 9 Vertical profiles of temperature (T), pH, specific conductivity (SC), dissolved oxygen (DO) and Eh and in the Filón Centro pit lake (Tharsis mine). The approximate locations of the chemocline, mixolimnion, and monimolimnion are also indicated. Data from March 2008

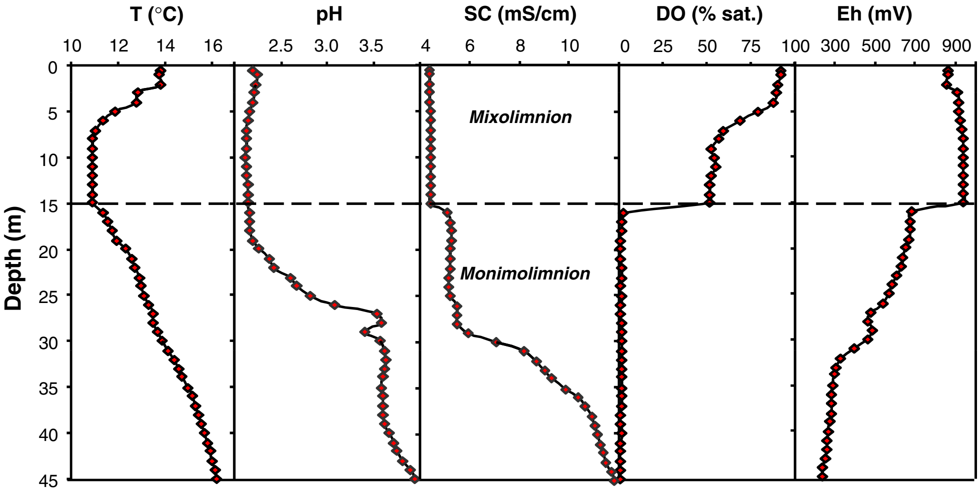

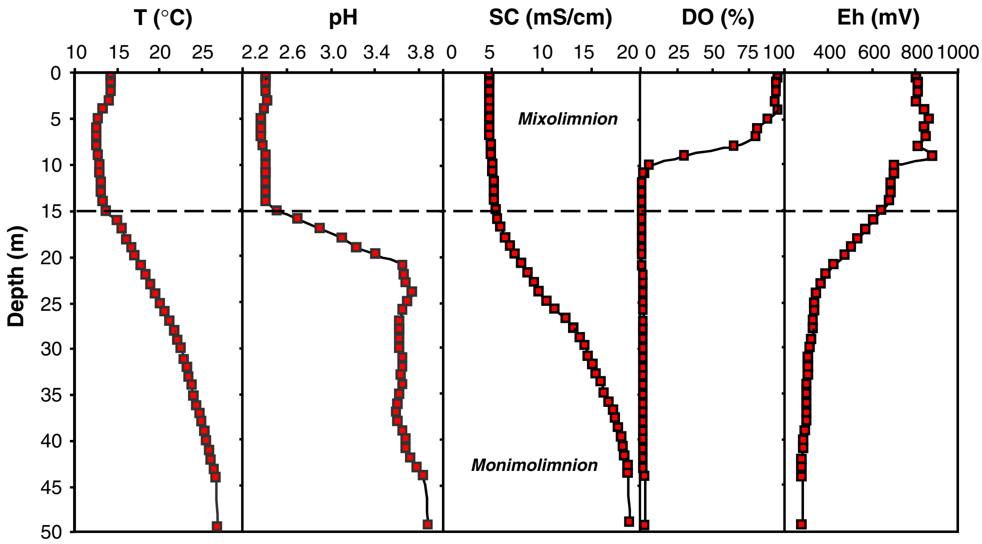

Fig. 10 Vertical profiles of temperature (*T*), pH, specific conductivity (*SC*), dissolved oxygen (*DO*) and Eh in the Guadiana pit lake (Herrerías mine). The approximate locations of the chemocline, mixolimnion, and monimolimnion are also indicated. Data from March 2008

usually adsorbed on these compounds (Sánchez-España et al. 2005a, b). Arsenic could be mobilized into the aqueous phase by desorption and/or direct re-dissolution of the solid phases. A similar process could result in releases of phosphate and organic carbon, both of which adsorb strongly onto freshly precipitated ferric oxides at low pH (e.g. Cameron et al. 2006; Spiteri et al. 2008; see references cited therein). Elevated concentrations of phosphate and TOC have been detected in mine drainage minerals in the IPB (0.10–0.30 wt% P_2O_5 and 0.40–1.40% C_{org}, Sánchez-España et al. 2006b, 2007b).

In addition to the biological processes discussed above, several abiotic processes must also be considered to account for the stratification of the IPB pit lakes, as well as the increase with depth of other metals (such as Zn) that do not partition into Fe(III)-sediments (Sánchez-España et al. 2005a, b, 2006a, b). Possible abiotic processes include: (1) subaqueous oxidation of pyrite by O_2 and/or Fe^{3+}; (2) acid dissolution of carbonate and aluminosilicate minerals on the pit walls; (3) changes in the history of progressive filling of the pit lakes; (4) influx of ground water; and (5) influx of mineralized water from flooded underground mine workings that are connected to the pit lakes. In the latter case, washing of large amounts of secondary, metal-rich sulphate salts accumulated in the mine workings could have strongly affected the water quality of the lakes. As well, the high temperatures (up to 27°C) near the bottom of the Herrerías pit lake can hardly be explained only by the heat released during bacterial oxidation of organic carbon. Because this pit lake is connected to an extensive system of underground galleries and shafts, it is possible that warm, high salinity water from the underground mines is migrating into the deep pit lake. A similar idea was proposed to help explain the elevated temperature and poor water quality of the monimolimnion of the Berkeley pit lake in Montana, USA (Davis and Ashenberg 1989; Gammons and Duaime 2006; Gammons et al. 2006). Regarding point 3 (above), progessive filling of pit lakes by waters of very different chemistry, density and/or temperature can be a key factor to develop meromictic conditions (Castendyk and Webster-Brown 2007). Detailed considerations of the flooding histories and ground water contributions to the IPB pit lakes are beyond the scope of this paper, and must await future studies.

An important difference between the Type I lakes (e.g. Confesionarios, San Telmo, and N^{a}S^a Carmen) and the Type II lakes (e.g. Cueva de la Mora, Herrerías, or Filón Centro) is the vertical profiles in iron concentration and redox speciation. Type I lakes typically show abundant ferric iron in their monimolimnia, despite the absence of detectable DO. For example, at Confesionarios, Fe(III) comprises 84–87% of the total iron in the upper monimolimnetic layer, and 12 to 25% in the lower layer (Fig. 11). In contrast, for Type II lakes, only ferrous iron exists in the monimolimnion. For Type I lakes, it is possible that pyrite remaining on the pit lake walls (or in the underground workings connected with the pit lake) could be undergoing some degree of subaqueous oxidation mediated by Fe^{3+} through the reaction:

$$FeS_2(s) + 14Fe^{3+} + 8H_2O \rightarrow 15Fe^{2+} + 2SO_4{}^{2-} + 16H^+ \tag{7}$$

Furthermore, because dissolved ferric iron is still abundant in the lower anoxic water layer of Confesionarios (Fig. 11), Fe^{3+}/ferric mineral reactions could be acting as an effective pH-buffering system of the pit lake water (e.g. through reaction 1). This buffering mechanism could explain the fact that the pH of the water is not so dramatically increased as in the above reported cases of Cueva de la Mora, Herrerías, and Filón Centro (although

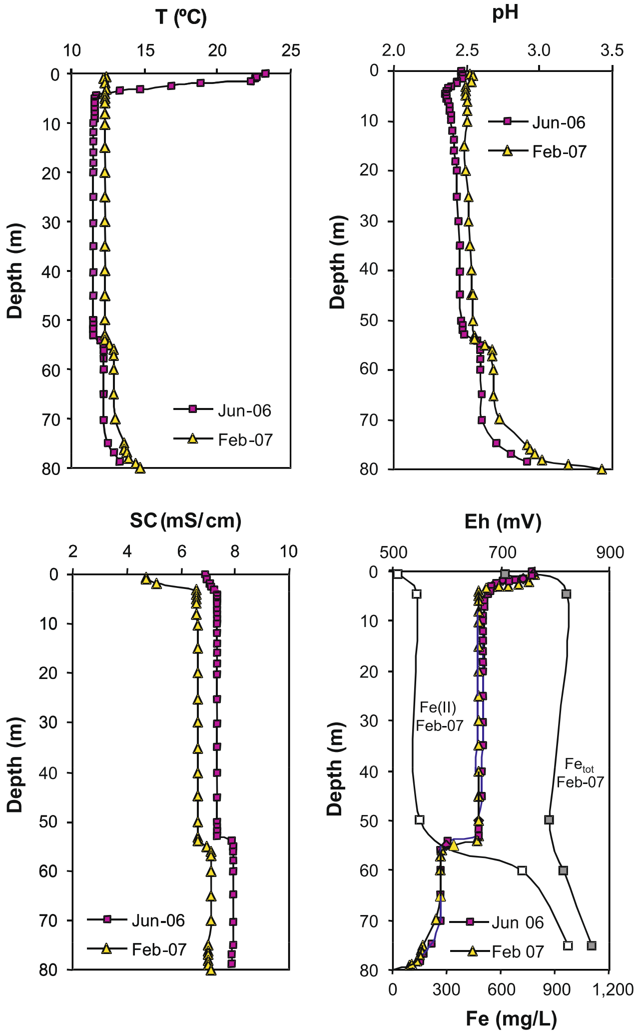

Fig. 11 Vertical profiles of temperature (*T*), pH, specific conductivity (*SC*), Eh and ferrous/total iron concentration [Fe(II)/Fe$_{tot}$] in the Confesionarios pit lake in June 2006 and February 2007. With the exception of the uppermost part of the water column, the small, systematic differences in the profiles could be due to the fact that different equipment was used to collect the two data sets

some proton consumption seems to be taking place near the water/sediment interface; Fig. 11).

The stratification patterns observed in the Type II pit lakes of Cueva de la Mora, Filón Centro, and Herrerías are rather unusual compared to most natural lakes (Wetzel 2001), as well as acidic mine pit lakes such as the Lusatian lignite mines in Germany (Friese 2004; Herzsprung et al. 1998) or the Berkeley pit lake in Montana, USA (e.g. Davis and Ashenberg 1989; Gammons and Duaime 2006; Pellicori et al. 2005). Salinity gradients with depth have been described in the monimolimnia of some other German open cast mining lakes, such as those of Soldbald Stassfurt or Rassnitzer See in the Merseburg–Ost area (Boehrer and Schultze 2008). However, several considerations make the pit lakes of the IPB exceptional examples of vertical discontinuity. Such factors include: (1) the vertical development of the monimolimnia (with thicknesses of 30–35 m, representing between 65 and 75% of the entire water column), and (2) the slope of the chemical and thermal gradients than can be observed downwards. The Confesionarios pit lake represents some kind of transitional case between Types I and II lakes in the IPB. The Confesionarios deposit was only mined by open-cast methods and, unlike Cueva de la Mora, Filón Centro, or Herrerías, does not have any shaft or underground mine gallery connected with the open pit. This means that hydrologic connection to underground workings is not a pre-requisite for development of gradational vertical profiles in the monimolimnia of the IPB pit lakes.

Cueva de la Mora: a singular example of double-diffusion convection in a mining pit lake?

One of the most unusual and interesting features of the vertical profiles for the Cueva de la Mora pit lake is the metric scale “staircase” pattern of homogenous water layers separated by sharp compositional and thermal boundary layers (Figs. 2, 3, 12). This type of stratification is diagnostic of water bodies that experience a phenomenon known as double-diffusion convection (DDC), and has been reported in polar oceans, the Black Sea, oceanic trenches, volcanic crater lakes such as lake Nyos (Cameroon), and other natural lakes (Kelley et al. 2003; Schmid et al. 2004; and references therein). DDC has been extensively studied in laboratory experiments with bottom-heated salt gradients and occurs when both temperature and salinity increase downwards in a manner such that the thermally induced density decrease is compensated by a density increase caused by a higher salinity (Kelley et al. 2003; Turner 1973, 1978). In contrast to other mixing processes, DDC results in an upwards flux of both salinity and heat, which results in discrete layers whose thicknesses can be calculated by semi-empirical equations (e.g. Fedorov 1988; Kelley 1984).

Cueva de la Mora may represent a singular example of DDC influencing the entire monimolimnion of a mining pit lake. Based on the profiles in Fig. 12, four different conductive layers can be recognized with thickness varying from 2 to 10 m. The boundary zones between these layers, which are 2–2.5 m thick, are characterized by strong gradients in salinity (Fig. 12). Although the staircase arrangement is stable throughout the year, the exact position of the steps and corresponding boundaries appear to migrate vertically with the seasons (Fig. 12), possibly due to climatic variations in temperature and rainfall. Although less pronounced, a staircase pattern is also observed in the vertical profiles of other parameters such as T, pH, and Eh (Fig. 2).

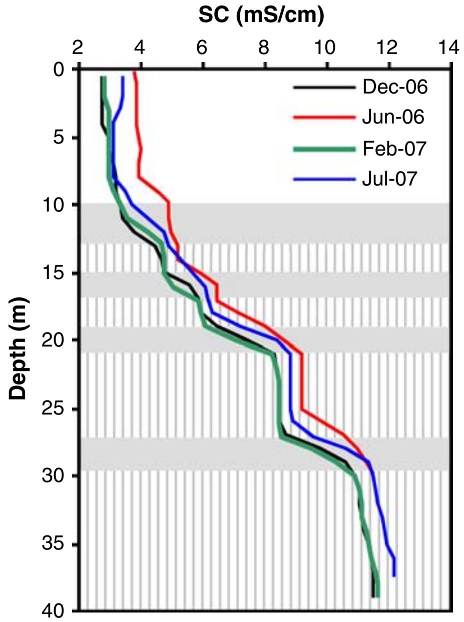

Fig. 12 Vertical distribution of successive layers in the pit lake of Cueva de la Mora. The regions with *vertical bars* (based on data from February 2007) denote homogenous layers of discrete SC values separated by boundary layers (*shaded regions*) of rapidly changing salinity. This type of staircase profile is diagnostic of double-diffusion convection (DDC)

Summary and conclusions

This study reports unusually pronounced vertical gradients of physico-chemical parameters for several pit lakes of the Iberian Pyrite Belt. In each case, a thin chemocline of only a few meters depth usually separates an upper, oxygen-saturated mixolimnion with very low pH (2.5–2.7) and relatively low metal concentrations from a lower, anoxic, moderately reducing, and chemically stratified monimolimnion. The monimoloimnia show marked downwards trends of decreasing redox potential, increasing temperature, increasing specific conductivity, and increasing pH. Concentrations of sulphate, metals, and metalloids also notably increase with depth. Some elements (e.g. Fe, As) reach concentrations in the deepest waters that are orders of magnitude higher than those at the surface. Especially interesting are the “staircase” vertical profiles observed in the lake at Cueva de la Mora, which may be caused by double-diffusive convection with a coupled upwards flux of heat and dissolved solids.

Various factors, both biotic and abiotic, are believed to contribute to the vertical stratification patterns observed in meromictic pit lakes of the IPB. Reductive dissolution of dissolved Fe^{3+} and ferric mineral phases coupled with the oxidation of organic matter in the water column and underlying sediment are most likely catalyzed by microbes. Additionally, bacterial reduction of SO_4^{2-} in pore waters within the sediment cover could be taking place. At this time, knowledge of these biogeochemical processes is still limited. Therefore, it is difficult to ascertain the degree at which the hypothetical microbial activity (including primary photosynthetic productivity and Fe(II)-oxidation in the mixolimnion, and C-decomposition and Fe(III) reduction in the pit lake bottom) may have contributed to the observed chemical configuration. Abiotic processes that could influence stratification patterns include pit lake morphometry, subaqueous oxidation of pyrite, dissolution of secondary salts, influx of ground water or mine water from flooded underground galleries, and changes in the history of flooding of each lake with waters of differing temperature and chemistry.

The reasons why lakes such as Cueva de la Mora, Herrerías, or Filón Centro have developed strong physico-chemical gradients towards the pit lake bottom, whereas other pit lakes, like San Telmo or N^{a}S^{a} Carmen, are chemically homogenized, still have to be resolved. Further research efforts are needed to solve this question, which has clear implications for the evaluation and design of possible remediation alternatives. Future studies to be conducted in the IPB pit lakes will include detailed chemical, mineralogical, and microbiological investigations of the sediment-water interface, along with stable isotopic studies of waters and minerals, geochemical modeling, and laboratory and field experiments aimed at revealing geochemical and microbiological controls on the pit lake composition.

Acknowledgments We are grateful to Dr M.A. Aguilera (Centro de Astrobiología, CSIC-INTA), who carried out a preliminary identification of eukaryotic microorganisms of the Cueva de la Mora pit lake, and provided images taken by confocal microscopy. We sincerely thank Professor Christopher Gammons for his helpful scientific and editorial comments made on an earlier version of this manuscript. The suggestions and critical revisions made by Ted Eary and an anonymous reviewer are also greatly acknowledged. We finally thank Bob Kleinmann for his kind assistance provided during the editorial handling. This work has been supported with funds provided by IGME through several research projects.

References

Aguilera A, Manrubia SC, Gómez F, Rodríguez N, Amils R (2006) Eukaryotic community distribution and its relationship to water physicochemical parameters in an extremely acidic environment, Río Tinto (Southwestern Spain). Appl Environ Microb 72–8:5325–5330

Bigham JM, Nordstrom DK (2000) Iron and aluminum hydroxysulfates from acid sulfate waters. In: Alpers CN, Jambor JL, Nordstrom DK (eds) Sulfate minerals: crystallography, geochemistry, and environmental significance, Rev Mineral Geochem, vol 40. pp 351–403

Bigham JM, Schwertmann U, Traina SJ, Winland RL, Wolf M (1996) Schwertmannite and the chemical modeling of iron in acid sulfate waters. Geochim Cosmochim Acta 60:2111–2121

Boehrer B, Schultze M (2008) Stratification of lakes. Rev Geophys 46:RG2005. doi:10.1029/2006RG000210

Braungardt CB, Achterberg EP, Elbaz-Poulichet F, Morley NH (2003) Metal geochemistry in a mine-polluted estuarine system in Spain. Appl Geochem 18:1757–1771

Cameron D, Willett M, Hammer L (2006) Distribution of organic carbon in the Berkeley pit lake, Butte, Montana. Mine Water Environ 25(2):93–99

Castendyk D, Webster-Brown J (2007) Sensitivity analyses in pit lake prediction, Martha Mine, New Zealand 1: relationship between turnover and input water density. Chem Geol 244:56–73

Davis A, Ashenberg D (1989) The aqueous geochemistry of the Berkeley Pit, Butte, Montana, USA. Appl Geochem 44:23–36

Ehrlich HL (2002) Geomicrobiology, 4th edn. Marcel Dekker, Inc., NY, p 768

Fedorov KN (1988) Layer thicknesses and effective diffusivities in “diffusive” thermohaline convection in the ocean. In: Nihoul JCL, Jamart BM (eds) Small-scale turbulence and mixing in the ocean. Elsevier, Amsterdam, pp 471–479

Friese K (2004) Depth distribution of heavy metals in lake sediments from lignite mine pit lakes of Lusatia (Germany). Stud Quaternaria 21:197–205

Gammons CH, Duaime TE (2006) Long term changes in the limnology and geochemistry of the Berkeley pit lake, Butte, Montana. Mine Water Environ 25:76–85

Gammons CH, Metesh JJ, Snyder DM (2006) A survey of the geochemistry of flooded mine shaft water in Butte, Montana. Mine Water Environ 25:100–107

González-Toril E, Llobet-Brossa E, Casamayor EO, Amann R, Amils R (2003) Microbial ecology of an extreme acidic environment, the Tinto river. Appl Environ Microbiol 6:4853–4865

Herzsprung P, Friese K, Packroff G, Schimmele M, Wendt-Potthoff K, Winkler M (1998) Vertical and annual distribution of ferric and ferrous iron in acidic mining lakes. Acta Hydrochim Hydrobiol 26:253–262

IGME (2008) Cortas inundadas de la Faja Pirítica: Inventario e hidroquímica. Memoria Final de Proyecto, Instituto Geológico y Minero de España, Ministerio de Ciencia e Innovación, Madrid, Spain, 281 pp. http://www.igme.es

Kelley DE (1984) Effective diffusivities within oceanic thermohaline staircases. J Geophys Res 89:10484–10488

Kelley DE, Fernando HJS, Gargett AE, Tanny J, Özsoy E (2003) The diffusive regime of double-diffusive convection. Prog Oceanogr 56:461–481

López-Archilla AI, Amils R (1999) A comparative ecological study of two acidic rivers in southwestern Spain. Microbial Ecol 38:146–156

López-Archilla AI, Marín I, Amils R (2001) Microbial community composition and ecology of an acidic aquatic environment: the Tinto river, Spain. Microbial Ecol 41(1):20–35

Nordstrom DK (1982) The effect of sulphate on aluminum concentrations in natural waters: some stability relations in the system Al_2O_3–SO_3–H_2O at 298 K. Geochim Cosmochim Acta 46:681–692

Olías M, Nieto JM, Sarmiento AM, Cerón JC, Cánovas CR (2004) Seasonal water quality variations in a river affected by acid mine drainage: the Odiel river (south west Spain). Sci Total Environ 333:267–281

Parkhurst DL, Appelo CAJ (1999) User’s guide to PHREEQC (Version 2)—a computer program for speciation, batch-reaction, one-dimensional transport, and inverse geochemical calculations. USGS WRI 99–4259. Denver, CO, USA

Pellicori DA, Gammons CH, Poulson SR (2005) Geochemistry and stable isotope composition of the Berkeley pit lake and surrounding mine waters, Butte, Montana. Appl Geochem 20:2116–2137

Regenspurg S, Brand A, Peiffer S (2004) Formation and stability of schwertmannite in acidic mining lakes. Geochim Cosmochim Acta 68:1185–1197

Rowe FO, Sánchez-España J, Hallberg K, Johnson DB (2007) Microbial communities and geochemical dynamics in an extremely acidic, metal-rich stream at an abandoned sulfide mine (Huelva, Spain) underpinned by two functional primary production systems. Environ Microbiol 9(7):1761–1771

Saez R, Pascual E, Toscano M, Almodovar G (1999) The Iberian type of volcano-sedimentary massive sulphide deposits. Miner Deposita 34:549–570

Sánchez-España J (2000) Mineralogy and geochemistry of the massive sulphide deposits of the northernmost sector of the Iberian Pyrite Belt (San Telmo-San Miguel-Peña del Hierro), Huelva, Spain. Ph.D. Thesis, University of the Basque Country (UPV-EHU), Bilbao, Spain, 301 pp

Sánchez-España J, López Pamo E, Santofimia E, Aduvire O, Reyes J, Barettino D (2005a) Acid mine drainage in the Iberian Pyrite Belt (Odiel river watershed, Huelva, SW Spain): geochemistry, mineralogy and environmental implications. Appl Geochem 20:1320–1356

Sánchez-España J, López-Pamo E, Santofimia E, Reyes J, Martín Rubí JA (2005b) The natural attenuation of two acidic effluents in Tharsis and La Zarza-Perrunal mines (Iberian Pyrite Belt, Spain). Environ Geol 49:253–266

Sánchez-España J, López-Pamo E, Santofimia E, Reyes J, Martín Rubí JA (2006a) The impact of acid mine drainage on the water quality of the Odiel river (Huelva, Spain): evolution of precipitate mineralogy and aqueous geochemistry along the Concepción-Tintillo segment. Water Air Soil Poll 173:121–149

Sánchez-España J, López-Pamo E, Santofimia E, Reyes J, Martín Rubí JA (2006b) Trace metal sorption onto schwertmannite and hydrobasaluminite: examples from the Iberian Pyrite Belt. Aquat Geochem 12:269–298

Sánchez-España J, Santofimia E, González Toril E, San Martín-Úriz P, López Pamo E, Amils R (2007a) Physicochemical and microbiological stratification of a meromictic pit lake (San Telmo, IPB). In: Cidu R, Frau F (eds) Proceedings of the IMWA symposium. Cagliari, Sardinia, Italy, pp 447–451

Sánchez-España J, López-Pamo E, Santofimia E (2007b) Iron terraces in acid mine drainage systems: a discussion about the organic and inorganic factors involved in their formation through observations from the Tintillo acidic river (Riotinto mine, Huelva, Spain). Geosphere 3(3):133–151

Sánchez-España J, López-Pamo E, Santofimia E, Diez-Ercilla M (2008a) The acidic mine pit lakes of the Iberian Pyrite Belt: an approach to their physical limnology and hydrogeochemistry. Appl Geochem 23:1260–1287

Sánchez España FJ, López-Pamo E, Diez M, Santofimia E (2008b) Monimolimnetic gradients in meromictic pit lakes of the Iberian Pyrite Belt: physico-chemical description. In: Rapantova N, Hrkal Z (eds) Proceedings of the IMWA 2008 Congress. Karlovy Vary, Czeck Republic, pp 567–570

Schlesinger WH (ed) (2005) Biogeochemistry. Treatise on geochemistry, vol 8. Elsevier Science, Oxford, p 720

Schmid M, Lorke A, Dinkel C, Tanyileke G, Wüest A (2004) Double-diffusive convection in Lake Nyos, Cameroon. Deep Sea Res Pt I 51:1097–1111

Spiteri C, Van Cappellen P, Regnier P (2008) Surface complexation effects on phosphate adsorption to ferric iron oxyhydroxides along pH and salinity gradients in estuaries and coastal aquifers. Geochim Cosmochim Acta 72–14:3431–3445

Tornos F (2006) Environment of formation and styles of volcanogenic massive sulphide: the Iberian Pyrite Belt. Ore Geol Rev 28:259–307

Totsche O, Pöthig R, Uhlmann W, Büttcher H, Steinberg EW (2003) Buffering mechanisms in acidic mining lakes—a model-based analyses. Aquat Geochem 9:343–359

Turner JS (1973) Buoyancy effects in fluids. Cambridge University Press, Cambridge, p 367

Turner JS (1978) Double-diffusive intrusions into a density gradient. J Geophys Res 83:2887–2901

Van Geen A, Boyle EA, Moore WS (1991) Trace metal enrichments in waters of the Gulf of Cádiz, Spain. Geochim Cosmochim Acta 55:2173–2191

Wetzel DB (2001) Limnology: lake and river ecosystems, 3rd edn. Academic Press, San Diego, p. 1006